Original Research Article

IMPACT OF TEMPERATURE ON BELITE CEMENT ADDITIVATED WITH NANOSILICA AND NANOALUMINA

A. Teixeira[a], N. Perez[a], A. Balza[b], O. Corona[b†*]

[a] Universidad Simón Bolívar, Sartenejas, República Bolivariana de Venezuela.
[b] PDVSA Intevep, S.A., Centro de Investigación y Desarrollo, Los Teques, República Bolivariana de Venezuela.
[†Current address] Instituto Superior de Formación Docente Salomé Ureña, República Dominicana

*Corresponding author, e-mail: oscarcorona78@gmail.com, (+1849) 9184892

Recibido: Junio 2018. Aprobado: Diciembre 2018.
Publicado: Diciembre 2018.

ABSTRACT
This research is an exploratory study that deals with the preparation, characterization, and evaluation of the influence of temperature on belite cement additivated with nano-silica and nano-alumina, as alternative cementitious material, with lower environmental impact and potential application in the process of oil well cementing. The aim was to identify the crystalline phases presents in the samples and the effect of temperature on their composition. Four blends were prepared: pure belite cement (B), belite cement with nanoalumina (BNA), belite cement with nanosilica (BNS) and a hybrid belite cement system (BH). The pastes were cured for 28 days at room temperature and the hardened materials were calcined at 110 °C and 200 °C and then characterized by x-ray diffraction, infrared spectroscopy, x-ray fluorescence spectroscopy, thermogravimetric analysis and scanning electron microscopy. The most relevant results revealed by x-ray diffraction analysis that the system B, exposed to 110 °C and 200 °C, showed the presence of α-C_2SH phase at 2θ = 17.25° and 29°. In contrast, the BNS and BNA systems did not show those peaks, which means that the absence of α-C_2SH phase is promoted for nanoadditives.

Keywords: Belite cement; eco-efficient cement; nanoalumina; nanosilica; green cements.

IMPACTO DE LA TEMPERATURA SOBRE LOS CEMENTOS BELÍTICOS ADITIVADOS CON NANOSÍLICE Y NANOALÚMINA

RESUMEN
Esta investigación consiste en un estudio exploratorio que aborda la preparación, caracterización y evaluación de la influencia de la temperatura en cementos belíticos aditivados con nanosílice y nanoalúmina, como material cementante alternativo, con menor impacto ambiental y potencial aplicación en el proceso de cementación de pozos de petróleo. El objetivo principal fue identificar las fases cristalinas presentes en las muestras y el efecto de la temperatura sobre su composición. Se diseñaron cuatro mezclas, cemento belítico puro (B), cemento belítico con nanoalúmina (BNA), cemento belítico con nanosílice (BNS) y cemento belítico híbrido (BH). Las pastas se curaron durante 28 días a temperatura ambiente. Los materiales endurecidos se calcinaron a 110 °C y 200 °C y luego se caracterizaron por difracción de rayos X, espectroscopía de infrarrojo, espectroscopía de fluorescencia de rayos X, análisis térmico y microscopía electrónica de barrido. Los resultados más relevantes por análisis de difracción de rayos X revelaron que el sistema B, expuesto a 110 °C y 200 °C, mostró la presencia de α-C_2SH en 2θ = 17,25° y 29°. En contraste, los sistemas BNS y BNA no mostraron ese pico, lo que significa que la ausencia de α-C_2SH es promovida por la presencia de estos nanoaditivos.

Palabras claves: Cementos belíticos; bajo impacto ambiental; nanoalúmina; nanosílice, cementos verdes.

INTRODUCTION

Cement is one of the most commonly used materials in the construction industry. In the oil well construction, cementing process has the purpose of providing an effective isolation between the pipe and sedimentary rock formation in order to prevent migration of fluids such as water or gas to another area or to the surface. Nowadays, this industry is facing great challenges in the exploration and production of oil and gas, reason why

unconventional processes are required to ensure exploitation of hydrocarbons. One of those is the secondary recovery of oil by thermal methods, subjecting the oil well at high temperatures and pressures, and promoting the decrease of the mechanical properties of hardened cement, it is because at 110 °C, the cement suffers the phenomenon of strength retrogression, wherein the main product of cement hydration, C-S-H gel, turns into α-dicalcium silicate hydrate (α-C_2SH), which has a crystalline structure, higher permeability and lower compressive strength (Figure 1) [1] [2].

On the other hand, the cement industry is considered as one of the most energy consumers, and it produces around 1.4 BT of CO_2 per year. For that reason, it is imperative the development of new technologies that involve a sustainable use of resources and energy, to comply with the Kyoto Protocol (Figure 2). Some alternatives are raised around the generation of new cementitious materials called green or eco-efficient cements [3].

Therefore, current needs in the oil and gas industry include the use of materials with high performance to enhance the useful life of oil wells and impacting on the reduction of CO_2 emissions.

The study of belite cements allow evaluating the possibility of replacing the Portland cement currently used, given that the manufacturing process involves a lower economic and environmental cost. The addition of silica and alumina nanoparticles promotes the acceleration of the hydration rate in belite cements, and then the increase in their early strength. Furthermore, decreasing the CaO/SiO_2 ratio helps to prevent undesirable phases formed at high temperature [4] [5].

This study addresses the preparation and characterization of alternative cement systems (synthetic belite cements), additivated with silica and alumina nanoparticles. The cement pastes were characterized by x-ray diffraction (XRD), infrared spectroscopy (FT-IR), x-ray fluorescence spectroscopy (XRF), thermogravimetric analysis (TGA), surface area analysis (by BET method) and high resolution scanning electron microscopy (SEM).

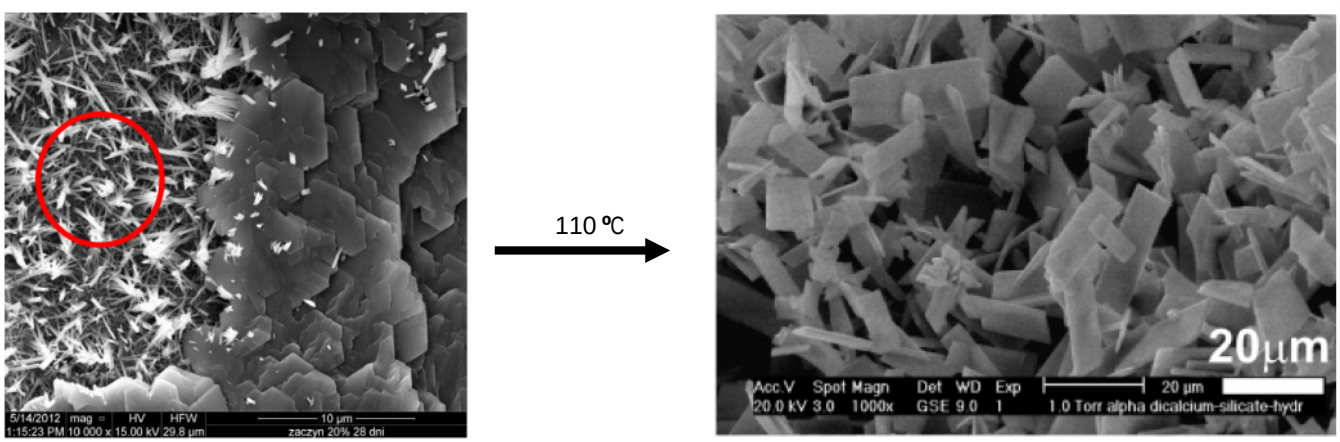

Fig. 1. Microstructures of C-S-H gel (left-red circle) and α-C_2SH phase (right) [6] [7].

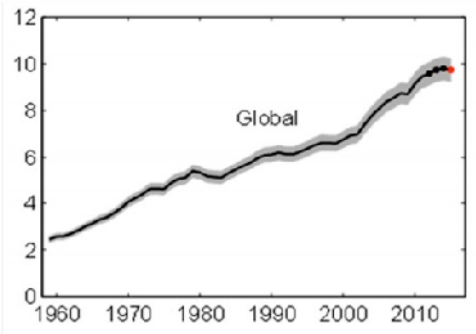

Fig. 2. Year-wise CO_2 emissions [GtC yr^{-1}] [8].

MATERIALS AND METHODS

The raw materials used in this work were β-C_2S phase from CTL Group (150 μm particle size and purity 99%). Nanoalumina (γ-Al_2O_3) and nanosilica (SiO_2) from mkNANO (15 nm particle size and purity 99.5%) Four admixtures of belite cement were designed (Table I), pure belite cement (B), belite cement with nanoalumina as addition (BNA), belite cement with nanosilica as a addition (BNS) and a hybrid belite cement (BH) formulation. All admixtures were prepared with deionized water, with a water/cement ratio of 0.5

Table I. Raw materials within each admixture.

Components [%]	B	BNA	BNS	BH
β-C_2S	100	100	100	100
Nanoalumina	-	0.5	-	0.5
Nanosilica	-	-	0.5	0.5

Pastes were poured into PVC moulds and cured for 28 days at room temperature (Figure 3). The hardened materials were pulverized and burned at 110°C and 200°C, while some samples were kept at room temperature. All the samples were characterized by x-ray diffraction (PANalytical, model X'Pert Pro), x-ray fluorescence spectroscopy (Bruker, model S2 Ranger), Fourier-transform infrared spectroscopy (Thermo Scientific, model Nicolet 6700) and thermal analysis (Netzsch, model STA 449 F3 Jupiter), whose primary goal was the identification of phases present in the different samples and the effect of temperature on them.

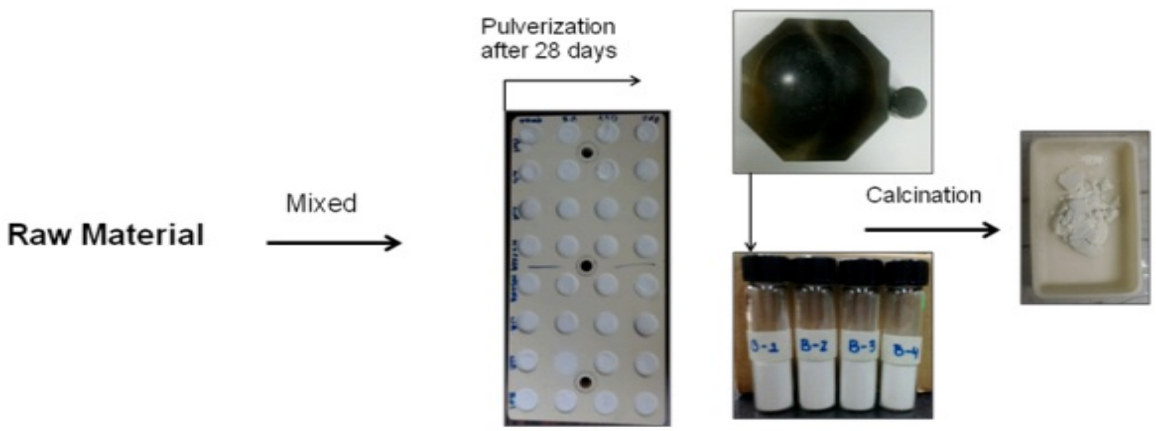

Fig. 3. Experimental setup.

RESULTS AND DISCUSSION

Fourier-Transform Infrared Spectroscopy (FTIR)

In figures 4 and 5, the FTIR analyses of B and BH systems are respectively shown. Results of BNS and BNA do not show because they are quite similar to BH and B, respectively. In both cases, the broad band from 3430 cm^{-1} to 3424 cm^{-1} moreover with the band at 1660 cm^{-1} correspond to asymmetrical stretching (ν_3), symmetrical stretching (ν_1) and bending (ν_2) vibrations of O-H groups in hydrated products. The band between 1418-1475 cm^{-1} presents a doublet due to the asymmetrical stretching (ν_3) of $[CO_3]^{2-}$, where the first, assigned to vaterite, is the predominant in both cases, except in B sample at 23 °C, where calcite is dominating. The bands at 902 cm^{-1}, 840 cm^{-1} and 518 cm^{-1} correspond to ν_3, ν_1 and ν_4 vibrations of Si-O bonding from non-hydrated C_2S. The strong band at 997 cm^{-1} is assigned to ν_3 vibrations of Si-O Q^2 tetrahedral (a tetrahedron of silicon connected to two others) in the structure of C-S-H gel. In the band at 748 cm^{-1}, it is noticed a shoulder assigned to ν_1 vibrations of Si-(OH) [9].

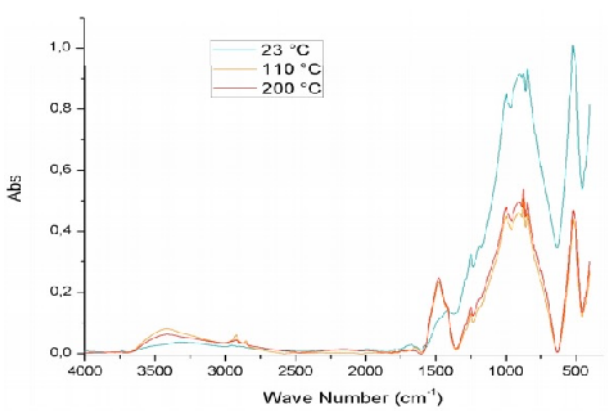

Fig. 4. . Infrared spectrum for B, exposed to different temperatures.

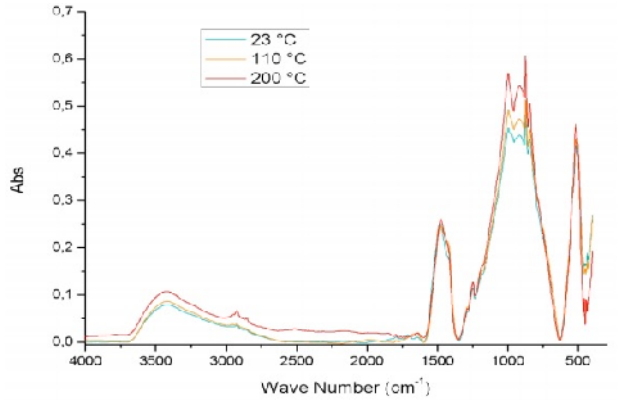

Fig. 5. Infrared spectrum for BH, exposed to different temperatures.

The main difference is in the broad band, where it is observed a higher intensity for BH system, as an indication that BH sample presents a higher hydration grade and therefore a larger amount of hydration products, which was also corroborated by the results of thermogravimetric analysis.

It is important to remark the difficulty of identifying the α-C_2SH phase, since its characteristic bands could be overlapped, by those located at 1278 cm^{-1} assigned to the vibration of -OH group bounded to Si, and the triplet of symmetrical stretch (ν_1) for O-H (Si), called *ABC triplet*, located at 2780 cm^{-1} (*A*), 2380 cm^{-1} (*B*) and 1715 cm^{-1} (*C*). From the above, the more intense band is *B*, which could be observed only in the sample B exposed at 200 °C as a slight bulge in the region between 2500 cm^{-1} and 1700 cm^{-1} (Figure 6) [10].

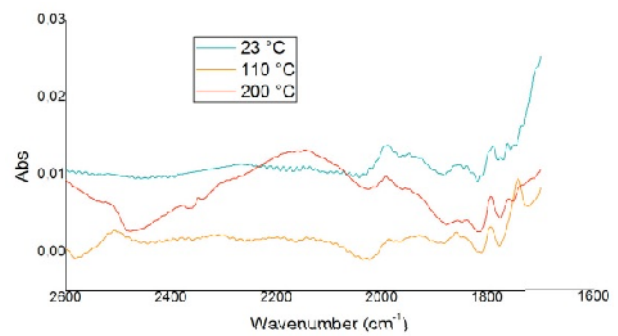

Fig. 6. Magnification of spectra in Figure 4 for the identification of *B* band in the *ABC* triplet.

X-ray diffraction (XRD)

In figures 7 and 8, it is highlighted the determined phases for B and BH cement systems, by the High Score Plus software, as well as additional phases, identified in previous studies by other researchers [11]. Patterns of BNS and BNA do not show because they are quite similar to BH. The main crystalline compounds observed are belite phase (β-C_2S), portlandite (CH) at 18° and calcite ($CaCO_3$) at 38,7°. In non-additivated belite cement samples, it was evidenced the presence of α-C_2SH at 110 °C and 200 °C for 2θ = 17.5°, 25° and 27°, which are the higher intensity peaks for α-C_2SH reported in literature [7]. These results corroborate those obtained by FTIR spectroscopy.

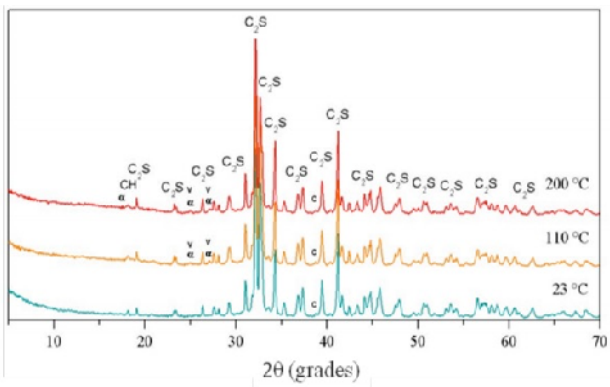

Fig. 7. Diffraction pattern of B, where α represent α-C_2SH, v=vaterite and c=calcite.

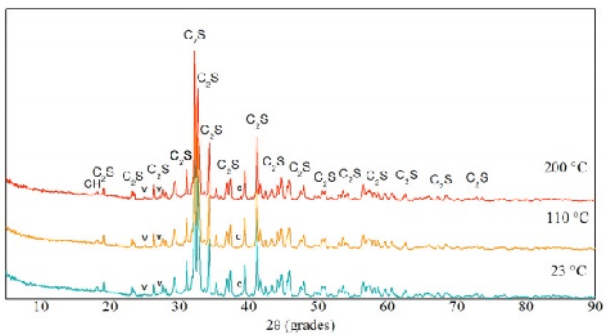

Fig. 8. Diffraction pattern of BH, where v = vaterite and c = calcite.

Thermal and x-ray fluorescence analysis.

By the thermogravimetric analysis (TGA), the percentage of mass loss versus temperature was determined, and in this way it was possible to estimate the amount of portlandite present in the samples. The percentage of calcium oxide (CaO) from it was determined to subtract it from the total percentage of CaO and to calculate the CaO/SiO_2 ratio of the C-S-H gel. Figure 9 shows thermograms obtained (upper in Figure 9), as well as the derivative of mass percentage (*d*TG) in the lower part.

The first mass loss is located between 100-300 °C, which corresponds to water losses from hydrated gels formed during the hydration of samples, two types of water occupy the pores and they are physisorbed or chemisorbed in the gels. According to the curve of the mass loss derivative (*d*TG), for this region, comparing the width of those peaks, it is possible to assert that there is a greater loss of mass for the sample BNS and BH in comparison with the BNA and B, it is also observed when the percentage of water released is analysed (Figure 10). This can be verified by infrared spectroscopy, where the samples of B and BNA show less hydrated gels than BNS and BH samples.

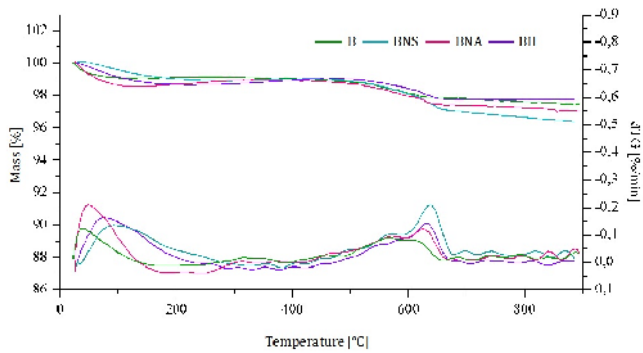

Fig. 9. Thermograms and *d*TG curves of the samples.

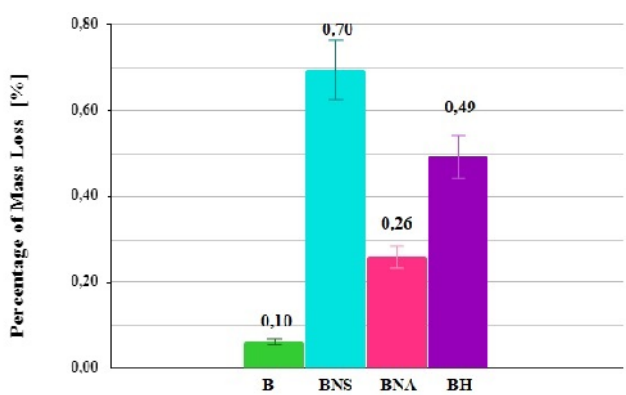

Fig. 10. Percentage of combined water in hydrated gels.

The second mass loss, located in the region between 550-900 °C, is assigned to the decomposition of calcium carbonate present in all the samples, releasing carbon dioxide (CO_2). This loss is due to the carbonation of the portlandite by reaction with atmospheric CO_2.

Assuming that all the portlandite formed during the hydration process suffered carbonation, then the amount of portlandite present in each sample was calculated applying stoichiometric ratios and the results are shown in Figure 11.

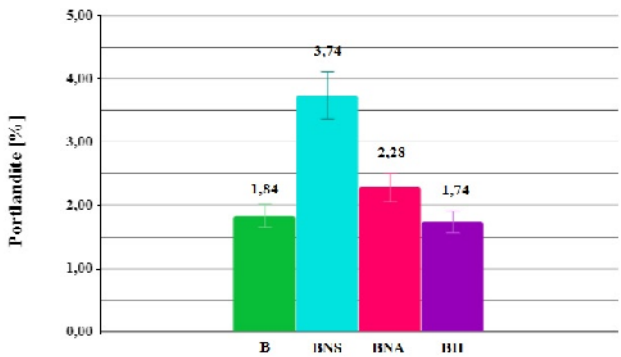

Fig. 11. Percentage of portlandite in all the samples.

Contrasting the results showed in Figure 11 with the percentage of mass loss graphed in Figure 10, it can be observed remarkable behaviours for each additivated system. On the one hand, nanoalumina in BNA sample seems to act as a retardant of hydration, since the amount of gels formed is less than the amount obtained in BNS sample, the same phenomenon is observed in terms of the percentage of portlandite. However, in both additivated systems the production of hydrated gels and portlandite is higher than the pure belite cement (B), and the explanation is the nucleation effect promoted by nanoparticles.

BH samples present an intermediate behaviour between because of the antagonism between nanoalumina and nanosilica. Nevertheless, the percentage of total portlandite for these samples represents the lowest value, which is a positive aspect because the presence of portlandite impact negatively on the durability of the cement [12].

Figure 12 shows the ratio between the percentage of hydrated gels and the percentage of portlandite produced, as a measure of pozzolanity. The behaviour observed is an indication that the nanoparticles also have a pozzolanic effect decreasing the amount of portlandite in the sample.

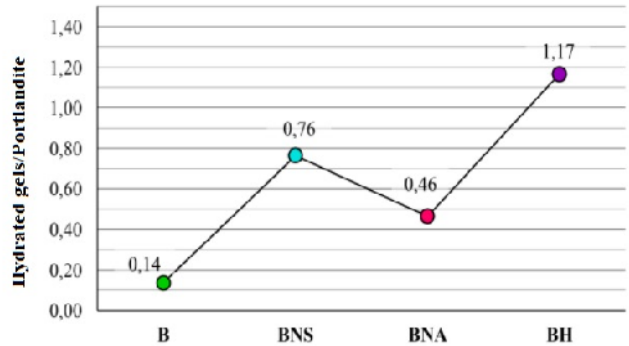

Fig. 12. Hydrated gels and portlandite ratio for belite cement systems.

It can be observed that the BH sample has the highest ratio followed by the BNS sample, so that the vaterite could actually be found around the surface of the portlandite preventing that the silica nanoparticles react with it, because the carbonation reaction takes place more rapidly than the pozzolanic reaction.

Furthermore, the BH sample has a lower percentage of portlandite, so the formation of vaterite is less favoured than in the case of BNS, due to this it can be said that the nanoparticles in the BH sample are less impeded than the of BNS in reacting with the portlandite to produce C-S-H, C-A-H or C-A-S-H gels.

Table II shows the percentages of oxides that typically are present in cements; they were determined by x-ray fluorescence (XRF) on each of the samples. Due to the very low amounts of nanoalumina (Al_2O_3) and nanosilica (SiO_2) added did not alter the CaO/SiO_2 (C/S) ratio. From these results and the thermogravimetric analysis, it is possible to determine C/S and C/(S + A) (Table III).

Table II. Percentage of oxides.

	K_2O	CaO	MgO	Fe_2O_3	Al_2O_3	SiO_2
B	0,0300	63,7800	0,9700	0,2100	0,0000	35,0100
BNS	0,0000	63,6600	0,8300	0,1100	0,0000	35,0100
BNA	0,0000	63,8200	0,9700	0,1100	0,0000	35,1000
BH	0,0300	63,5400	0,8800	0,1000	0,0000	35,4500

Table III. C/S and C/(S + A) ratios.

	CaO/SiO_2	$CaO/(SiO_2+Al_2O_3)$
B	1,78	1,78
BNA	1,77	1,77
BNS	1,74	1,74
BH	1,76	1,76

In the graph of C/S ratio as a function of temperature (Figure 13), it can be seen that the presence of α-C_2SH phase is very probable in the samples exposed to 110 °C. Typically, Portland cements have C/S ratio around 2.5, and at this value is expected the formation of undesired phases from 110 °C. Therefore, belite cements represent a better option for high temperature cements applications because, even without the addition of additives, it is possible to obtain C/S ratios in ranges where the formation of adverse phases is not promoted. This effect is enhanced by the addition of nanosilica and nanoalumina, thus effectively preventing the phenomenon of thermal retrogression.

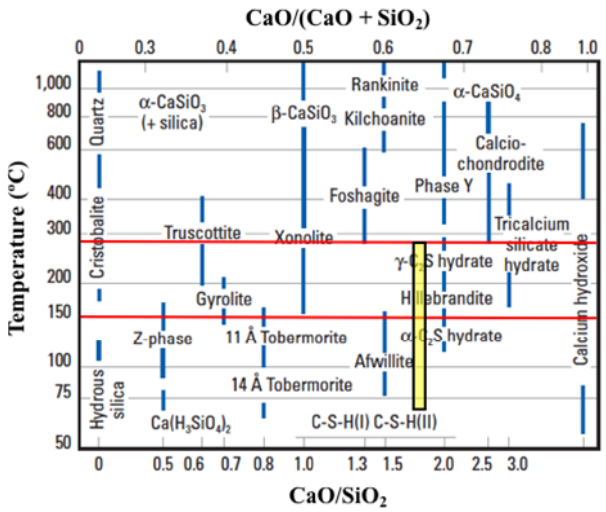

Fig. 13. In yellow the C/S ratio for belite cement systems studied at 100 °C and 200 °C.

Specific surface area analysis by N_2 adsorption Brunauer-Emmett-Teller method (SSA N_2-BET)

Figures 14 and 15 show the adsorption isotherms (BET isotherms) obtained for the samples B and BNA, respectively. Those corresponding to the samples BNS and BH are not shown in this section because they are very similar to B.

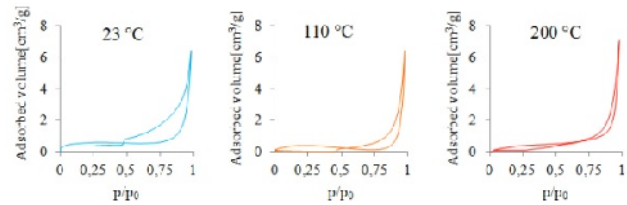

Fig. 14. BET isotherms for samples B at 23 °C, 110 °C and 200 °C.

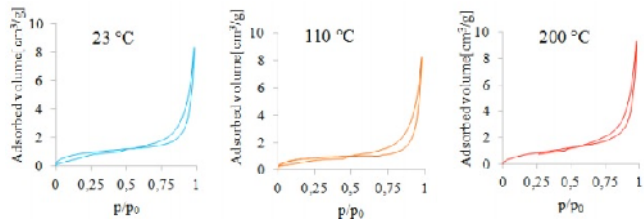

Fig. 15. BET isotherms for samples BNA at 23 °C, 110 °C and 200 °C.

According to IUPAC, the isotherms of Figures 14 and 15 resemble one of type IV, which is characteristic of mesoporous solids (2nm <size of Pore <50nm) [12].

Figure 14 clearly shows that the hysteresis loop of the samples exposed at room temperature is different from those exposed at 110 ° and 200 °C. At 23 °C, the cycle is type H3, according to the IUPAC classification, which is usually found in solids with pores in the form of plates or sharp particles of irregular size and shape. For the other samples, at 100 °C and 200 °C, the hysteresis cycle is type H1, which is characteristic of solids with aggregates or agglomerates of spheroidal particles of uniform size and shape [13]. These characteristics of the isotherms are due to the increase in the exposure temperature, where the loss of plate shape from the pores to the more uniform ones is promoted. However, the BNA system shows the same H1 hysteresis cycle for the different

temperatures, and then the temperature does not affect the shape or size of the pores in this kind of sample.

From the isotherms, the BET surface area can be obtained (Figure 16).

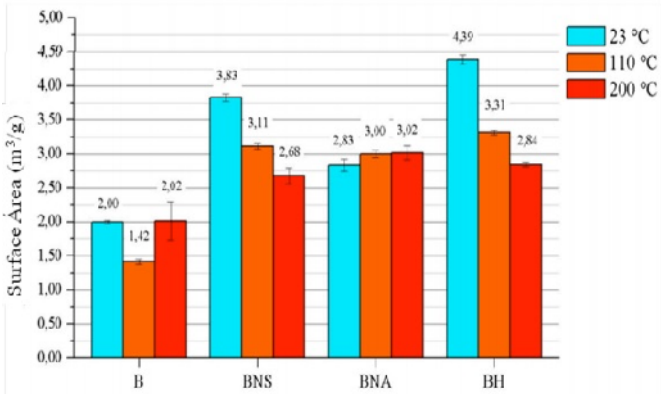

Fig. 16. SSA for cement systems studied at 23 °C, 110 °C and 200 °C.

Pure belite cement system (B) exposed at 110 °C has a smaller surface area than the same kind of sample exposed at room temperature. This is due to a process of dehydration of the gels, that occurs when the sample is subjecting to temperatures above 105 °C. In this process the volume of the C-S-H gel decreases and the total porosity of the sample increases [14]. At 200 °C an increase occurs, and it can be related to the appearance of α-C_2SH phase, since the cement matrix increase both the porosity and the permeability, therefore its specific surface area. All BNS samples have a larger surface area than B, which is due to the incorporation of nanosilica, which implies growth nuclei and a larger amount of hydrated gels, so that its surface area increases.

On the other hand, a progressive decrease of this property is observed while increasing the time of exposure to high temperatures, which is related to the dehydration process as is the case of sample B at 110 °C. However, the difference for the BNS system is that, because of silica nanoparticles, the dehydration process generates an internal environment called *autoclave effect*, favouring the pozzolanic reaction and therefore promoting the formation of hydration products (C-S-H and portlandite). In consequence, the densification of the system occurs, which could result in better mechanical properties, and it would be confirmed by scanning electron microscopy analyses. [15] [16]. BNA samples showed a contrasting behaviour with both BNS and B. Their surface area increase while the time of exposure to temperature increases, remaining invariable at higher temperatures. Therefore, it is possible to state that the gels of the BNA samples have a higher thermal stability compared to the other systems (C-A-H and/or C-A-S-H).

Scanning electron microscopy (SEM)

Scanning electron microscopy analyses were carried out on samples exposed at 200 °C, pure belite cement system (B) and the hybrid system (BH) which has both nanoalumina and nanosilica additives, in order to establish the microstructural differences of C-S-H gels in each case. Additionally, the presence of the α-C_2SH phase in sample B was confirmed, as well as vaterite and portlandite crystalline structures.

Figure 17 shows a hydrated grain of B system at different magnifications and its EDS analysis for chemical characterization. An amorphous gel was identified, which has morphology of irregular flakes, and it was also possible to determine the presence of carbonates, specifically vaterite polymorph (Figure 18). In this way, the results obtained by FTIR and XRD were supported.

On the other hand, Figure 19 shows the presence of the α-C_2SH phase in B samples exposed at 200 °C, thus corroborating the results obtained by FTIR, XRD and XRF for this system. According to Figure 19, the microstructure of α-C_2SH phase consists of thin sheets of rectangular layers, which agrees with the reported by Genvilas et.al [17].

Figure 20 shows the morphology analysis of C-S-H gel obtained for BH system. It was possible to distinguish an acicular and much denser structure than the reported for the system B (Figure 21). Hence, the results obtained by BET-SSA were confirmed.

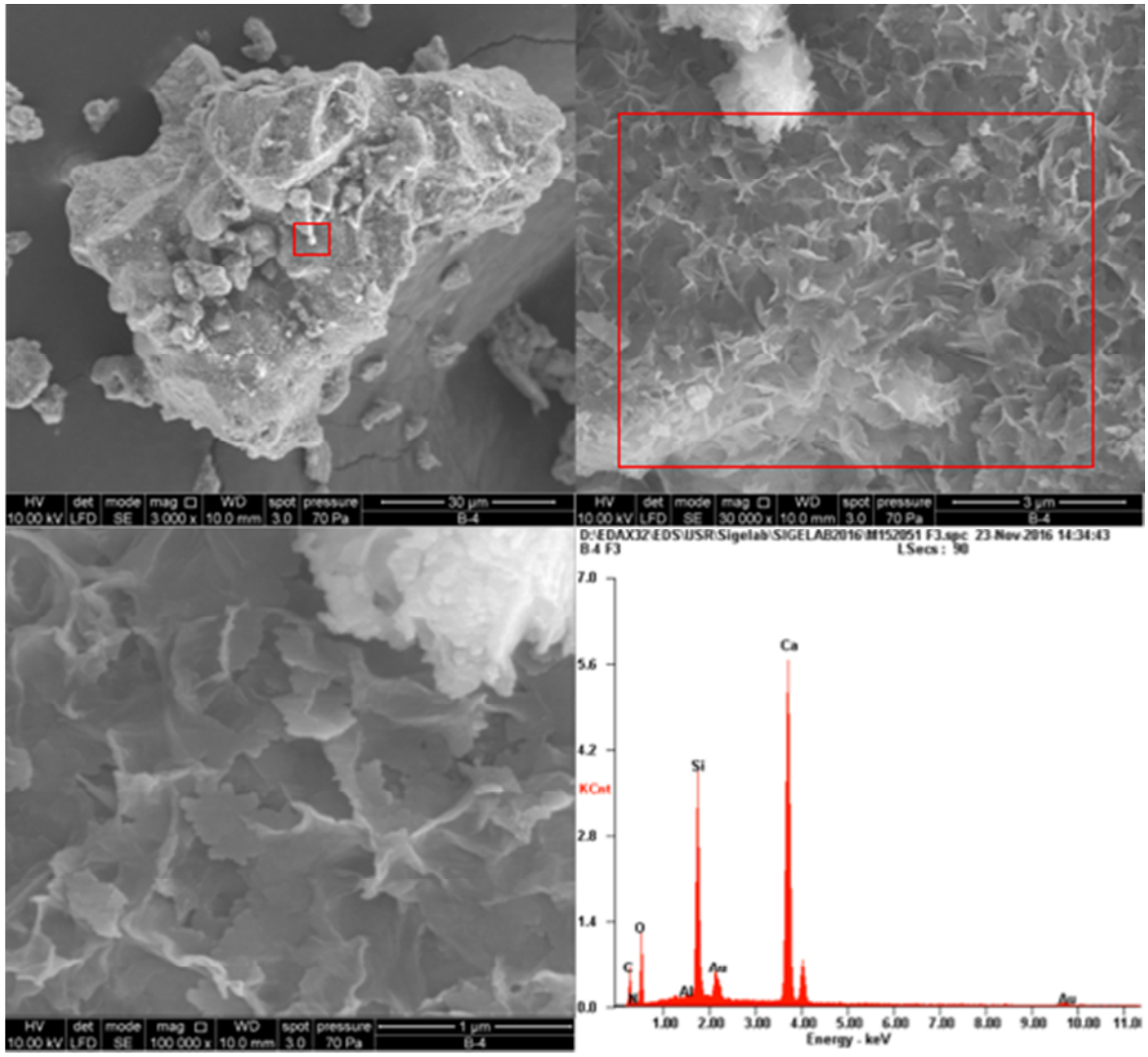

Fig. 17. SEM analysis of B sample exposed at 200 °C.

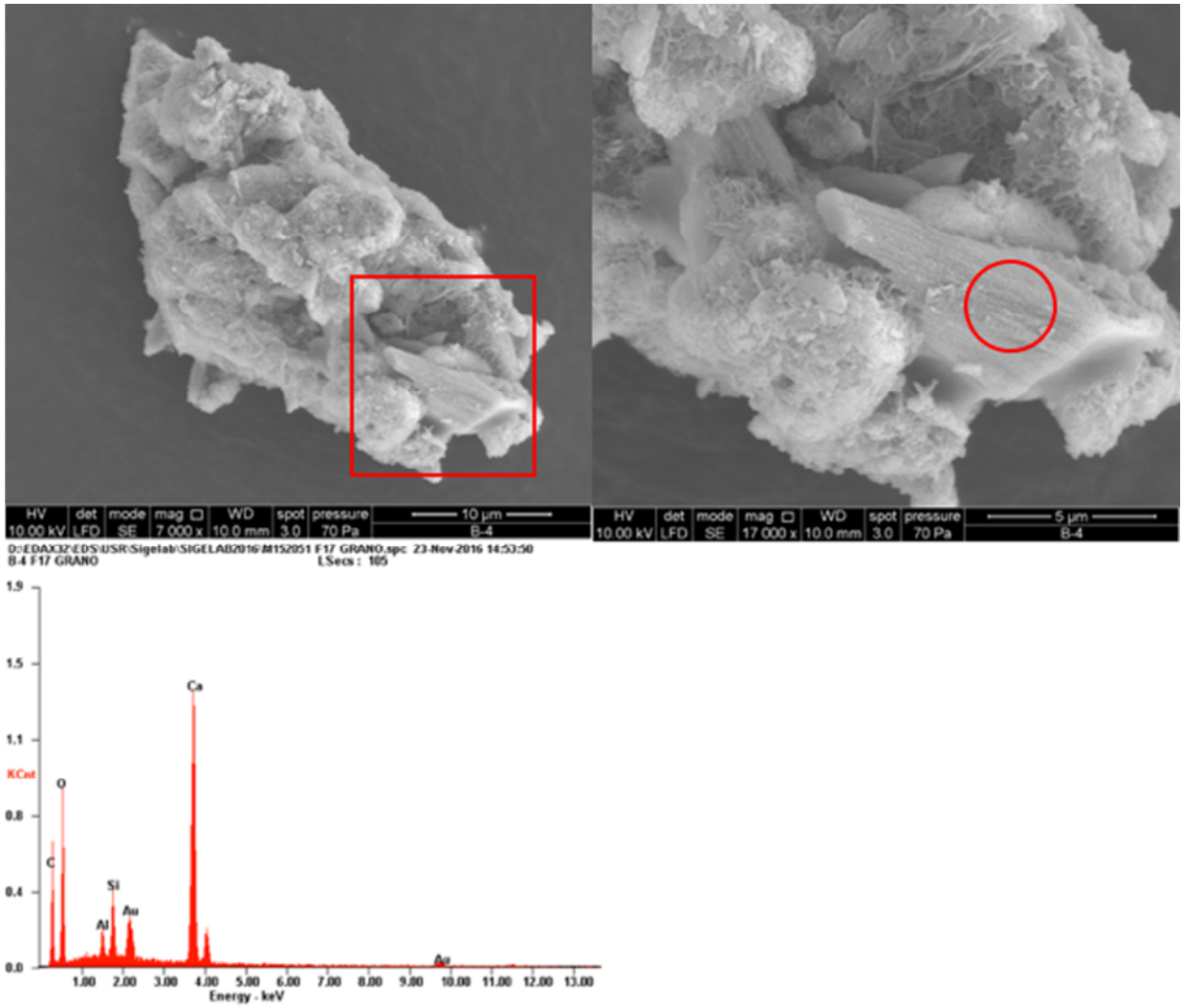

Fig. 18. Vaterite morphology and chemical characterization in B system at 200 °C.

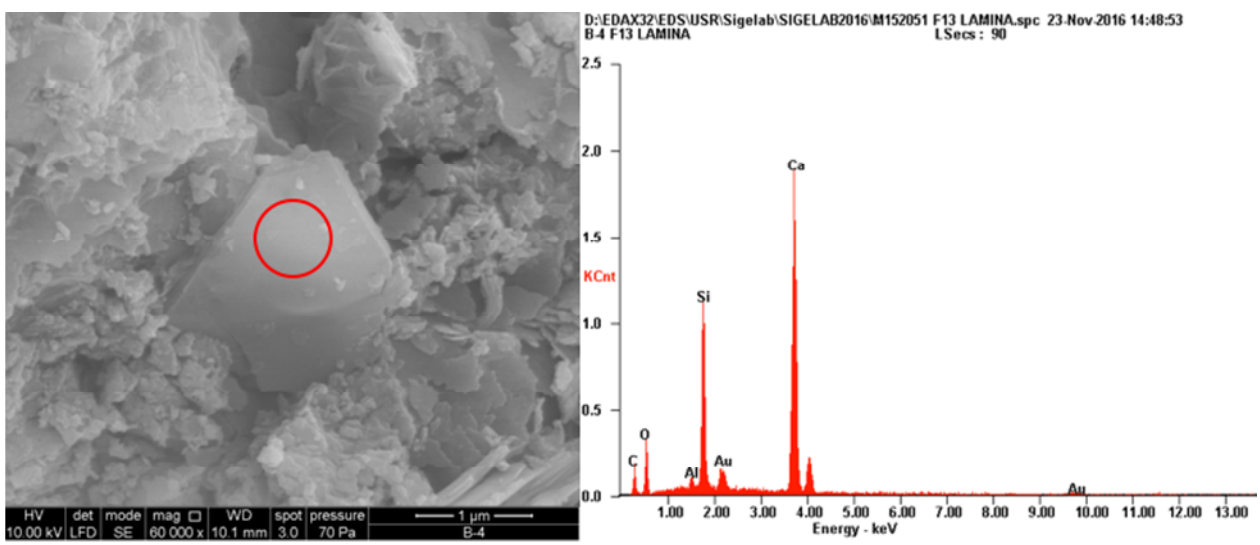

Fig. 19. SEM-EDS characterization of α-C_2SH phase within B sample at 200 ° C.

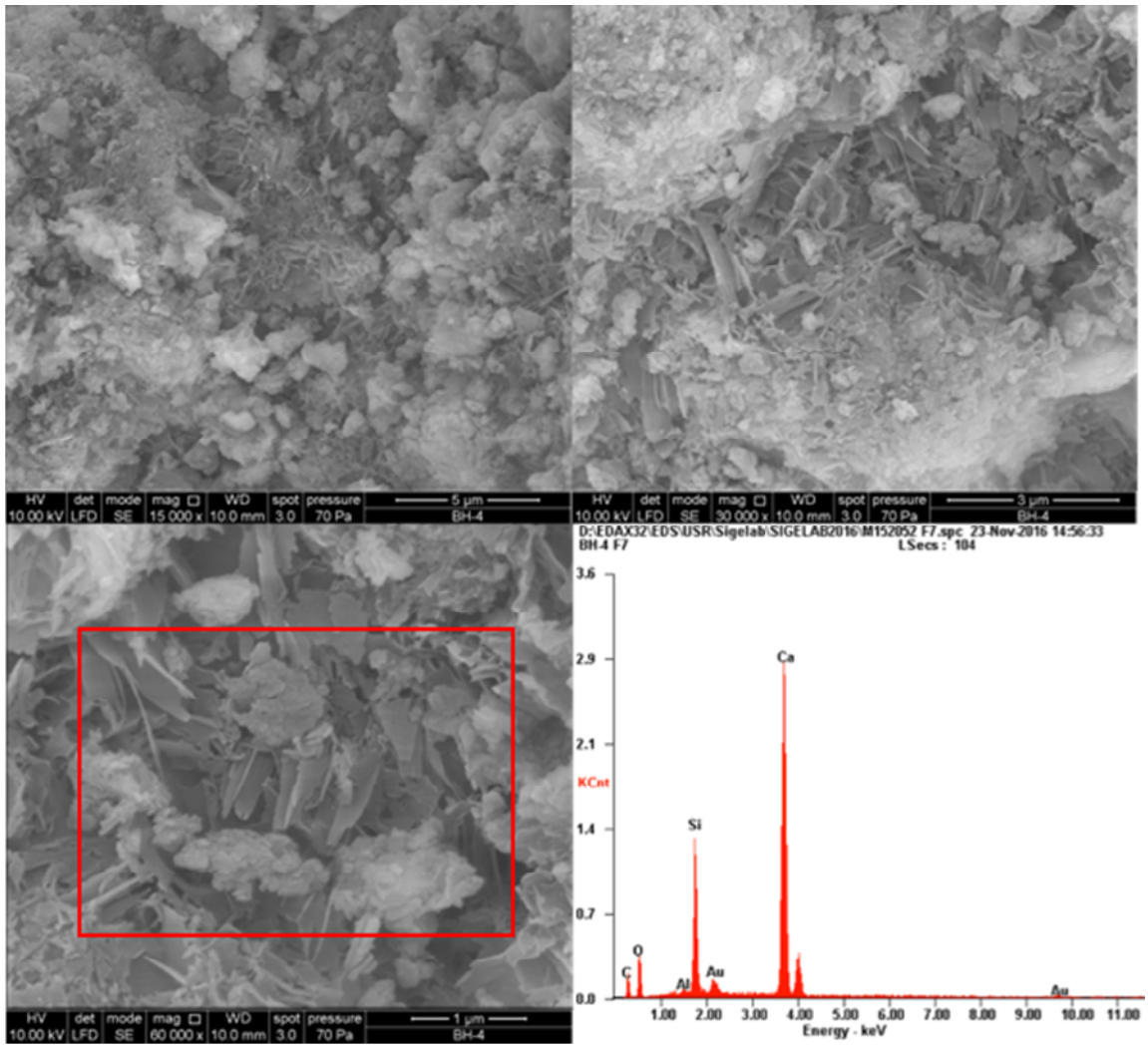

Fig. 20. Morphology and chemical characterization in BH system at 200 °C.

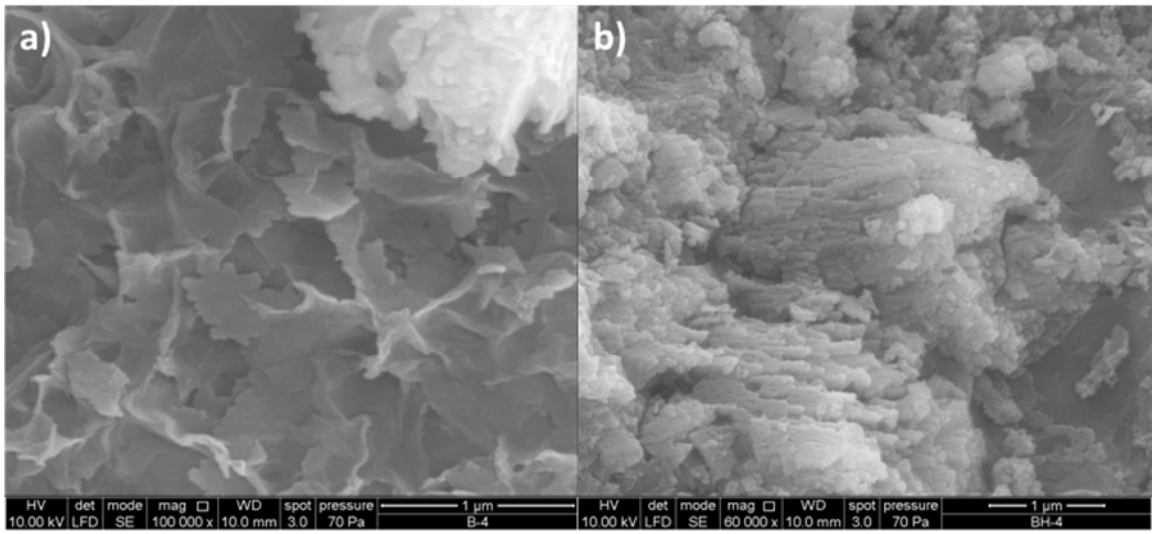

Fig. 21. Morphology of C-S-H gels: a) in the reference system (B) and b) in the hybrid system (BH), both samples exposed at 200 °C.

CONCLUSIONS

In this study the presence of the α-C_2SH phase was evidenced only in samples of non-additivated belite cement.

BNA system showed fewer amounts of C-S-H gels and portlandite in comparison with BNS, it confirmed the retarding effect of nanoalumina. However, the gels produced from the hydration of BNA (C-A-H and C-A-S-H) had a higher thermal stability.

Vaterite phase proved to be the predominant calcium carbonate polymorph in all samples excepting for the pure belite cement sample (B) at 23 °C, both the temperature and the presence of greater amount of portlandite seems to stabilize this polymorph.

Finally, the hybrid system (BH) is shown as the one with highest potential to be used in the cementing process of oil wells due to its low content of portlandite and the densification of microstructure at high temperatures.

ACKNOWLEDGEMENT

Thanks to PDVSA Intevep for the financial support and Abraham Salazar, Thomas Oropeza, Blas Delgado, Omar Ocanto and Manuel Olivo for their advice and knowledge along this research.

REFERENCES

[1] Barrios M. J. (2011) "Evaluación de la factibilidad de implementación de la inyección alternada de vapor de agua con gas en la faja petrolífera del Orinoco mediante el uso de un simulador numérico." Universidad de Oriente, Barcelona, Venezuela.

[2] Bezerra U.T., Martinelli A. E., Melo D. M. A., Melo M. A. F., Oliveira V. G. (2011) "The strength retrogression of special class Portland oil well cement." *Cerâmica* 57:150-154.

[3] SINIA, "Sistema Nacional de Información Ambiental." 3 August 2016. [on line]. Available: http://www.sinia.cl/1292/w3-article-48407.html.

[4] Guerrero A., Goñi S., Moragues A., Dolado J. S. (2005) "Microstructure and Mechanical Performance of Belite Cements from High Calcium Coal Fly Ash." *J. Am. Ceram. Soc*. 88:1845-1853.

[5] Land G., Stephan D. (2015) "Controlling Cement Hydration with Nanoparticles." *Cem. Concr. Compos* 57: 64-67.

[6] Diamond S. (1986) "The Microstructures of cement paste in concrete", 8th ICCCC. Vol. 1 pp. 113-121, Rio de Janeiro

[7] Garbev K., Gasharova B., Beuchle G., Kreisz S., Stemmermann P. (2008) "First Observation of α-$Ca_2[SiO_3(OH)](OH)$-$Ca_6[Si_2O_7][SiO_4](OH)_2$ Phase Transformation upon Thermal Treatment in Air." *J. Am. Ceram. Soc*. 91(1): 263-271.

[8] Le Quéré C., Moriarty R. (2015) "Global Carbon Budget 2015." *Earth Syst. Sci. Data*, 7:349-396

[9] Fernández L., Torrens D., Morales L. M., Martínez S. (2012) "Infrared Spectroscopy in the Analysis of Building and Construction Materials." of *Infrared Spectroscopy-Materials Science, Engineering and Technology*, InTech, pp. Chapter: 19.

[10] Garbev K., Gasharova B., Stemmermann P. (2014) "A Modular Concept of Crystal Structure Applied to the Thermal Transformation of α-C2SH." *J. Am. Ceram. Soc*. 97(7): 2286-2297.

[11] V. Rodrigues. (2015) "Efecto puzolánico de nanopartículas de alúmina en la hidratación de fases de clinker Portland," Universidad Simón Bolívar, Caracas. Available at: http://159.90.80.55/tesis/000171107.pdf

[12] Chartterjee A. K. (1996) "High belite cements-present status and future technological options: part I." *Cem. Concr. Res.* 26(8): 1213-1225.

[13] Leofanti G., Padovan M., Tozzola G., Venturelli B. (1998) "Surface area and pore texture of catalysts" *Catal. Today* 41(1-3):207-219.

[14] Zhang Q., Ye G., Koenders E. (2013) "Investigation of the structure of heated Portland cement paste by

using" *Construction and Building Materials,* 38:1040–1050.

[15] Balza A., Corona O., Alarcón A., Echevarrieta J., Goite M., González G. (2016) "Estudio Microestructural del Cemento Portland aditivado con Nanomateriales" *Acta Microscopica,* 25(1):39-47.

[16] Heikal M., Ismail M. N., Ibrahim N. S. (2015) "Physico-mechanical, microstructure characteristics and fire resistance of cement pastes containing Al_2O_3 nano-particles" *Construction and Building Materials.* 91: 232–242.

[17] Genvilas R., Siauciunas R.. (2015) "The Influence of Temperature and Nature of CaO Component on theFormation of α-C_2SH" *Solid State Phenomena,* 244:12-18.